

Article

Design of a Dead-Time Compensator Robust H_∞ State Feedback Temperature Controller for a Precalciner of a Cement Rotary Kiln

José Salcedo-Hernández ^{1,*} , Raul Rivas-Perez ^{1,2,*}  and Javier Sotomayor-Moriano ¹ 

¹ Departamento de Ingeniería, Pontificia Universidad Católica del Perú (PUCP), Avenida Universitaria 1801, San Miguel, Lima 15088, Peru; jsotom@pucp.edu.pe

² Departamento de Automática y Computación, Universidad Tecnológica de la Habana José Antonio Echeverría (CUJAE), La Habana 19390, Cuba

* Correspondence: jose.salcedo@pucp.edu.pe (J.S.-H.); rivas@automatica.cujae.edu.cu (R.R.-P.)

Abstract: A dead-time compensator robust H_∞ state feedback controller (DTC- H_∞ -SFC) for the temperature control in a precalciner of a cement rotary kiln is designed. A mathematical model of the process under study with ARMAX structure was obtained. A dead-time compensator robust H_∞ state feedback controller is therefore designed. The results of the comparative evaluation of the DTC- H_∞ -SFC vs. DTC+PI designed controllers showed that the DTC- H_∞ -SFC gives improved performance of the control system.

Keywords: robust H_∞ state feedback controller; dead-time compensator; systems identification; precalciner; cement rotary kiln



Citation: Salcedo-Hernández, J.; Rivas-Perez, R.; Sotomayor-Moriano, J. Design of a Dead-Time Compensator Robust H_∞ State Feedback Temperature Controller for a Precalciner of a Cement Rotary Kiln. *Appl. Sci.* **2022**, *12*, 2594. <https://doi.org/10.3390/app12052594>

Academic Editor: Muhammad Junaid Munir

Received: 26 January 2022

Accepted: 27 February 2022

Published: 2 March 2022

Publisher's Note: MDPI stays neutral with regard to jurisdictional claims in published maps and institutional affiliations.



Copyright: © 2022 by the authors. Licensee MDPI, Basel, Switzerland. This article is an open access article distributed under the terms and conditions of the Creative Commons Attribution (CC BY) license (<https://creativecommons.org/licenses/by/4.0/>).

1. Introduction

At present, the cement industry is developing an increasing level of automation [1,2]. Increased automation has been motivated by the new demands of this industry for high-performance in terms of cement quality, productivity, efficiency, and lower costs in production and maintenance [3].

Likewise, in the last few decades, universal cement output has increased significantly, in emerging and non-emerging states. Consequently, studies related to increasing the efficiency of the productive process in this industry are highly relevant to today's scientific interest [4–6].

Cement manufacturers face major challenges. First, they must master increasingly stringent environmental regulations because it is an industry with rather high carbon dioxide emissions and secondly, they face increasing pressure to reduce costs due to excessive competition worldwide [7–9].

The key apparatus used in this industry is the rotary kiln [10], which is an enormous, slightly inclined cylinder that gradually turns on its axis, moved by a powerful electrical motor, while its content (the raw meal) is heated to extremely high temperatures (1350–1500 °C) [11]. The raw meal is loaded at the kiln superior end and moves toward the burner flame located at the inferior end as the kiln rotates. The high temperature occasions the raw meal to react and this reaction creates the clinker [10].

Once the clinker is manufactured, it is chilled quickly to minimize the creation of a glass phase and guarantee the maximum yield of alite (tricalcium silicate) formation, a vital component for the cement hardening properties [11].

After cooling, to produce powdered cement, the clinker nodules are ground with approximately 5% gypsum and other minor mineral additives to the consistency of powder [5]. Therefore, clinker manufacturing is of significant value [10].

Different approaches have been proposed in recent decades concerning the modelling [12–14] and control of cement rotary kilns [15–17].

In most modern cement factories, rotary kilns are equipped with a cyclone preheater, a precalciner, and a cooler [18–20]. The cyclone preheater consists of a vertical tower containing a series of cyclones stages with an auxiliary combustion system (precalciner) located at the bottom of the preheating tower to increase the temperature of the raw meal before putting it in the rotary kiln [10]. Raw meal enters the precalciner [21].

The preheater heats the raw meal using warm scape fumes from the rotary kiln, while the precalciner provides additional heat to the raw meal until it reaches a temperature between 860 °C and 950 °C, producing the decarbonizing process. This process is highly dependent on temperature and directly affects energy consumption [22]. It is well known that up to 70% of the energy consumption during the clinker manufacture process in modern rotary kilns is produced in the precalciner [23].

The decarbonizing process of the raw meal is one of the most important processes in the manufacturing of clinker, which is based on the endothermic calcination reaction [11]. The decarbonized raw meal then come in the rotary kiln where the clinker is produced [10].

Currently, the control and optimization of the precalciner temperature plays a vital role within the cement manufacturing process [24,25]. If poor temperature control is performed in the precalciner, a modification is generated in the grade of decarbonizing of the raw meal that enters the kiln affecting the rank of the clinker without the option of offsetting it in its entirety in the later stages of the production process [20]. This generates large material losses due to the damages produced in the refractory of the rotary kiln owing to the temperature increase and generates higher maintenance and production costs [26,27].

The precalciner is characterized by its ability to improve thermal efficiency and reduce heat waste in the cement kilns [11]. However, a deficient control leading to an excessive rise in temperature can cause high fuel consumption and generate high pollution by emitting toxic gases into the environment [28]. Consequently, effective temperature control in the precalciner is decisive to guarantee a high-quality clinker and efficient energy use [29].

Currently, the precalciner temperature control is mainly carried out using conventional PID controllers [24,30,31]. However, the dynamic performance of the precalciner is characterized by non-linear behaviour, time delays [32,33], parameter uncertainties, as well as large disturbances [34,35]. Thus, the precalciner is categorised as process with complex dynamic behaviour [36,37].

It is well-known that when processes have complex behaviours, the PID must perform well, see, e.g., [38–40]. Moreover, processes with time delays are problematic to control by conventional controllers due to control system instability [41–43]. Accurate control of these processes is very important [44–46].

These arguments constitute a strong motive for the design of advanced controllers [47,48] that will enable effective temperature control in the precalciner, as well as improve the clinker production process, reduce damage to mechanical equipment, increase the quality of the powdered cement and reduce energy-consumption and environmental pollution.

The dead-time compensator robust H_∞ state feedback control (DTC- H_∞ -SFC) is a novel advanced control technique that could greatly contribute to the improvement of productive processes because it combines the advantages of the robust H_∞ state feedback control with the advantages of the dead-time compensator (Smith predictor) [49–51]. A review of time delay control systems and of the Smith predictor control system can be found in [52,53].

Robustness is of vital significance in controller design, since real industrial processes are susceptible to external disturbances, measurement noises, and unmodelled plant dynamics [54–56].

The objective of this work is to design a DTC- H_∞ -SFC controller for the operative temperature control in a precalciner of a cement rotary kiln.

The DTC- H_∞ -SFC controller harnesses a mathematical model of the controlled process to compute control signals through the state feedback, which allows the controller to develop while taking into account only the free part of the process model without the time delay because the time delay is removed from the state feedback [57,58].

Unlike the PID controllers, the DTC- H_∞ -SFC controller shows a certain insensitivity to disturbances that take place in the productive processes allowing for a compensation of the time delay effect in the feedback.

Among the characteristics of the DTC- H_∞ -SFC controller is the need to have an accurate process model and continuous feedback on the state of the system to achieve closed-loop stability [59,60]. A benefit of this controller is the option of having state feedback and output feedback [61]. A sequence of controller actions is estimated and these are computed considering the process dynamics. The first component of the sequence becomes a reference point of the actuator element. If the system receives new sensor measurements, the calculation is repeated, and a new sequence is estimated.

The key results of this paper are the following: (1) A mathematical model that accurately described the temperature in a precalciner is obtained; (2) A DTC- H_∞ -SFC controller for the operative temperature control in a precalciner is developed.

This paper is planned as follows. In Section 2, a mathematical model of the process studied is obtained using systems identification techniques, and the design of the DTC- H_∞ -SFC controller is developed. Section 3 shows the discussions of the attained results. Lastly, a few conclusions are given in Section 4.

2. Materials and Methods

2.1. Identification of the Temperature Dynamic Behaviour in a Precalciner

The precalciner considered in this paper is the cement rotary kiln precalciner of the Cementos Lima company, Peru.

In this paper a DTC- H_∞ -SFC controller for the operative temperature control is designed. For the design of this controller, it is necessary to own a mathematical model that adequately depicts the temperature behaviour in the precalciner under study. However, obtaining a phenomenological model, based on the physical laws is very difficult due to the complex dynamic behaviour of the precalciner [35,37].

Currently, the system identification constitutes a potent tool for attainment adequate mathematical models of the dynamic behaviour of productive processes, see, e.g., [38,62]. For this reason, in this paper, the systems identification procedures are used to obtain an adequate mathematical model of the temperature dynamic behaviour in a precalciner based on the real time data observed (measured) of its input/output variables.

The precalciner considered is equipped with a temperature sensor (TT), a fuel flow sensor (FT), and a control valve of the fuel flow entering the precalciner burner. In addition, the cement rotary kiln has a SIMATIC S7-300 PLC and a control station (industrial PC) that is provided with a SCADA system for the supervision of the entire productive process, which facilitates the data collection and storage.

For the evolution of the system identification experiments, we considered as the input variable (manipulated) the variation of the fuel flow ($Q_f(t)$) that feeds the burner of the precalciner ($u(t)$) and as output (controlled) variable the temperature variation of exhaust gasses of the precalciner $y(t)$. This process is affected by disturbances, such as the raw flour flow variation to the precalciner, the fuel calorific value, the air temperature, etc.

In Figure 1 the experimental arrangement under operating conditions carried out for the data collection of the considered precalciner in open loop is shown, where PLC is the Programmable Logic Controller, PC is the Personal Computer, TT is the temperature transmitter, and TF is the fuel flow transmitter.

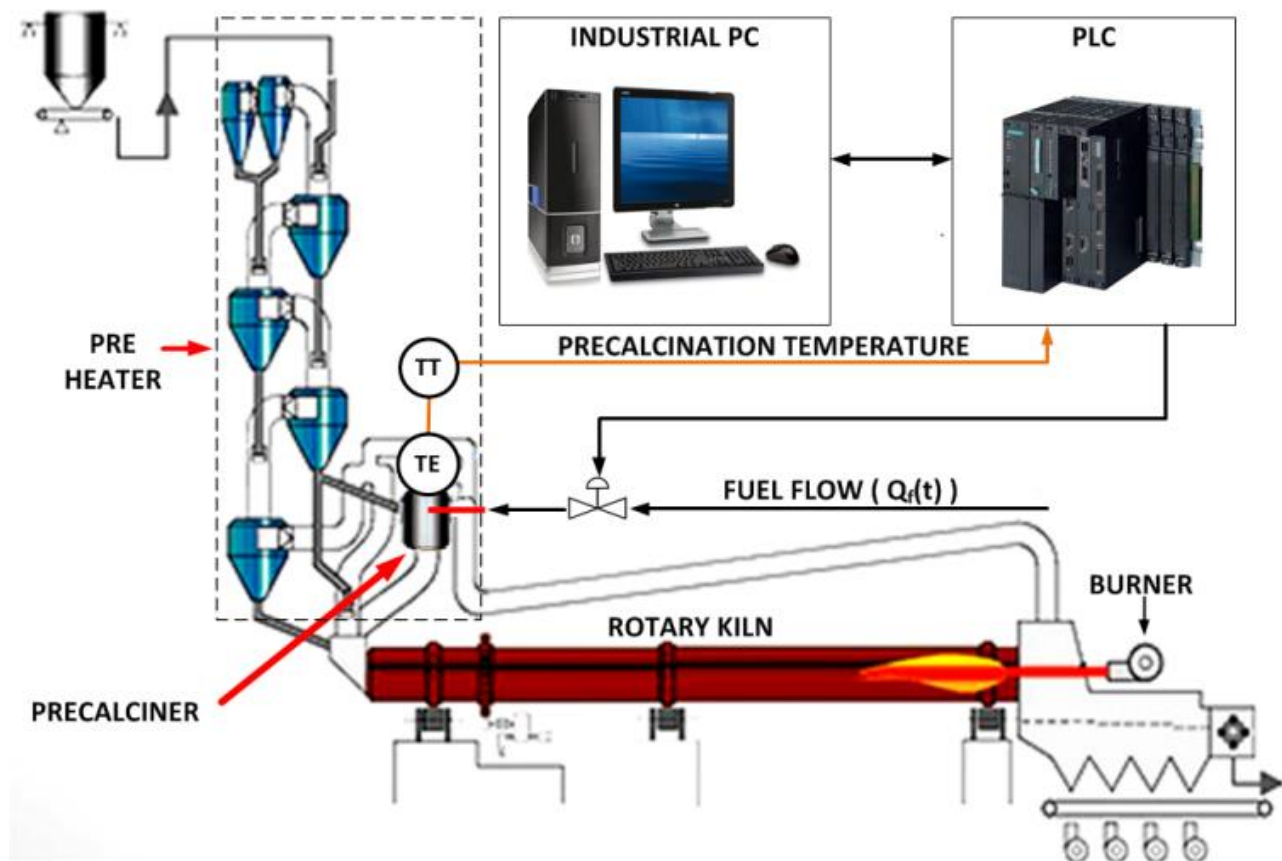


Figure 1. Diagram of the data collection in the precalciner.

For the development of a mathematical model of temperature in a precalciner, a pseudo-random binary sequence (PRBS) as input was applied [62].

The data were sampled with a sampling period $T_s = 60$ s. The data collected were separated into data for estimation and data for validation, and are displayed in Figure 2.

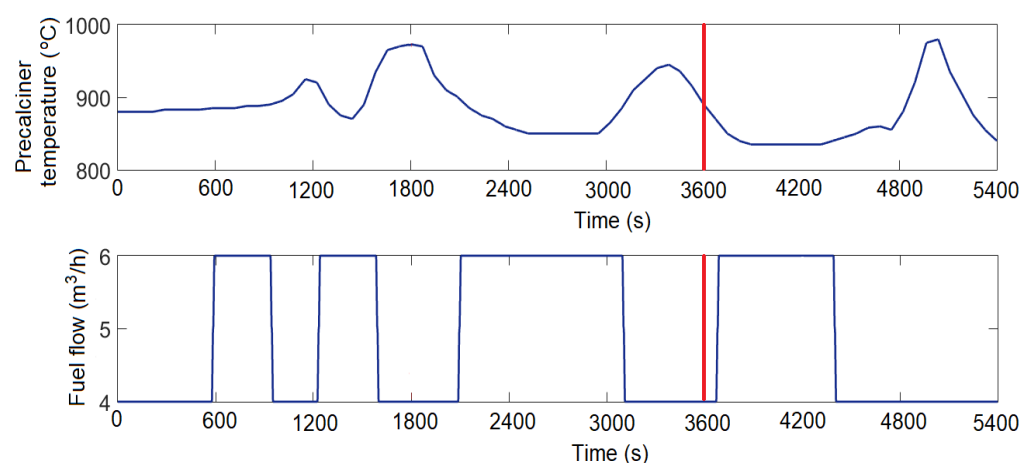


Figure 2. Results of the experiment with a pseudo-random binary sequence (PRBS).

Some discrete model structures (ARX, OE, Box-Jenkins and ARMAX) with dissimilar model orders were evaluated to decide which of them better depicted the temperature in the precalciner.

The estimation of the parameters was developed by means of the Prediction Error framework [62]. The parameters were computed for diverse model orders and time delays.

2.2. Model Validation

The model validation was performed based on the cross-validation method [62]. The model that better replicated the temperature behaviour in the precalciner was selected by quantifying the degree of accuracy with respect to the validation data. This was carried out by mean of a performance index (*FIT*), which was attained by the following expression [62].

$$FIT = \left[1 - \frac{\|y - \hat{y}\|}{\|y - \bar{y}\|} \right] * 100\% \quad (1)$$

where $y(t)$ is the measured output, $\hat{y}(t)$ is the estimated output, and $\bar{y}(t)$ is the mean of $y(t)$. The obtained validation results are shown in Table 1.

Table 1. Validation results.

Model Structure	Model Order						Performance Index(FIT)
	na	nb	nc	nd	nf	nk	
ARMAX	4	4	4	-	-	10	90.04%
BJ	-	4	4	4	4	9	86.72%
ARX	4	4	-	-	-	10	84.25%
OE	-	2	-	-	2	11	85.45%

Table 1 exhibits that the better attained model is a fourth-order model with ARMAX structure and time delay, which is characterized by the expression [62]:

$$y(t) = \frac{B(q)}{A(q)} q^{-nk} u(t) + \frac{C(q)}{A(q)} e(t) \quad (2)$$

where:

$$A(q) = 1 - 1.783q^{-1} + 0.0356q^{-2} + 1.729q^{-3} - 0.5489q^{-4} \quad (3)$$

$$B(q) = 19.91q^{-1} - 46.14q^{-2} + 33.1q^{-3} - 6.842q^{-4} \quad (4)$$

$$C(q) = 1 - 1.164q^{-1} - 0.109q^{-2} + 0.5668q^{-3} - 0.2937q^{-4} \quad (5)$$

and $e(t)$ is the uncorrelated random white noise with zero mean.

The validation results of the mathematical model attained are shown in Figure 3 and depict a high adjustment index (FIT).

The obtained discrete-time mathematical model (1) of the precalciner temperature can, thus, be characterized by the next transfer function with dominant time delay:

$$G(z) = \frac{19.91z^3 - 46.14z^2 + 33.1z - 6.842}{z^4 - 1.783z^3 + 0.0356z^2 + 1.279z - 0.5489} z^{-10} \quad (6)$$

2.3. Design of a DTC-H ∞ -SFC Controller

The H ∞ controller design is a current and active research area [49,63,64]. From its beginnings to the present there has been made substantial growth in this field [50,51,54]. It has been extensively proposed to solve diverse complex industrial and academic control problems [55–57]. In this paper H ∞ -based robust controller is proposed to solve the problem of operative temperature control in a precalciner.

The control system is characterized agreed to configuration showed in Figure 4, where P is the generalized plant or interconnected system, w represents all the external inputs, that includes reference signal and disturbances, z denoted the output signals to be to minimized (consisting of all error signals), y is the vector of measurements available to the controller K , and u is the vector of control signals [57,59]. The measured variable y is used in K to calculate the control signals u ($u = Ky$).

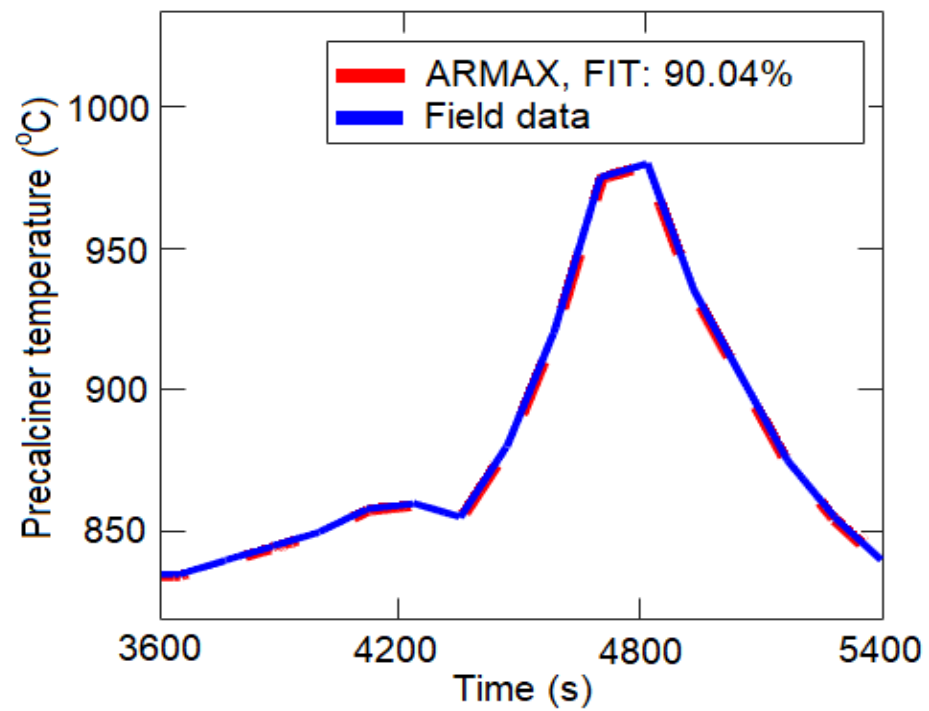


Figure 3. Validation results.

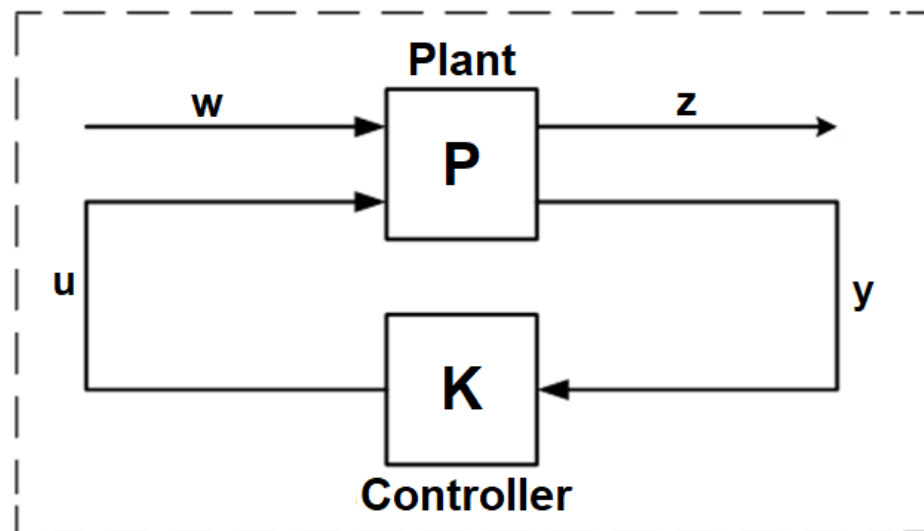


Figure 4. Standard diagram of the robust H_∞ configuration.

The controller design trouble is to meet a stabilizing controller K that produces a signal u regarding the information from y to decrease the effect of w on z , minimizing the closed loop norm from w to z [50]. It is correspondent to minimizing the H_∞ -norm of the transfer function from w to z [51].

The generalized plant P is partitioned as:

$$P = \begin{bmatrix} P_{11} & P_{12} \\ P_{21} & P_{22} \end{bmatrix} \quad (7)$$

Therefore, the control system can be represented as:

$$\begin{bmatrix} z \\ y \end{bmatrix} = P \begin{bmatrix} w \\ u \end{bmatrix} = \begin{bmatrix} P_{11} & P_{12} \\ P_{21} & P_{22} \end{bmatrix} \begin{bmatrix} w \\ u \end{bmatrix} \quad (8)$$

From (8) it is obtained:

$$\begin{aligned} z &= \begin{bmatrix} P_{11} + P_{12}K(I - P_{22}K)^{-1}P_{21} \end{bmatrix} w \\ z &:= F_l(P, K) \end{aligned} \quad (9)$$

where $F_l(P, K)$ is the lower linear fractional transformation of P and K [50]. Thus, the controller design objective becomes [51]:

$$\min_{K \text{ stabilizing}} \|F_l(P, K)\|_{\infty} \quad (10)$$

where the expression (10) is denoted as the H_{∞} optimization problem [55].

However, in industrial controller design it is enough to meet a stabilizing controller K , such that the H_{∞} -norm of the closed-loop transfer function is minor than a given positive number γ [50,57]:

$$\|F_l(P, K)\|_{\infty} < \gamma \quad (11)$$

where $\gamma > \gamma_0 := \min_{K \text{ stabilizing}} \|F_l(P, K)\|_{\infty}$

The H_{∞} controller commonly uses a state-space model to obtain the control signals $u(k)$ [65]. Therefore, from the derived model in z -domain of the precalciner temperature (6), the following process model was obtained in discrete-time states-space with time delay:

$$\begin{aligned} x(k+1) &= Ax(k) + B_1w(k) + B_2u(k-nk) \\ z(k) &= C_1x(k) + D_{11}w(k) + D_{12}u(k-nk) \\ y(k) &= C_2x(k) + D_{21}w(k) + D_{22}u(k-nk) \end{aligned} \quad (12)$$

where $x(k) \in \mathbb{R}^n$ is the state vector, $w(k) \in \mathbb{R}^p$ is the disturbance input, $u(k) \in \mathbb{R}^m$ is the control input, $y(k) \in \mathbb{R}^r$ is the measurement, $z(k) \in \mathbb{R}^q$ is the controlled output, nk is the discrete-time delay, A , B_1 , B_2 , C_1 , C_2 , D_{11} , D_{12} , D_{21} , D_{22} are matrices appropriately dimensioned,

$$A = \begin{bmatrix} 1.783 & -0.0356 & -1.279 & 0.5489 \\ 1 & 0 & 0 & 0 \\ 0 & 1 & 0 & 0 \\ 0 & 0 & 1 & 0 \end{bmatrix}, B_1 = B_2 = \begin{bmatrix} 8 \\ 0 \\ 0 \\ 0 \end{bmatrix}, C_1 = \begin{bmatrix} 0 & 0 & 0 & 1 \end{bmatrix},$$

$$C_2 = \begin{bmatrix} 2.489 & -5.768 & 4.138 & -0.8552 \end{bmatrix}, D_{11} = [0], D_{12} = [1], D_{21} = [1], D_{22} = [0],$$

$nk = 10T = 600$ s is the time delay.

Figure 5 shows the diagram of the precalciner temperature control system with the proposed DTC- H_{∞} -SFC controller, where $Y_{m1}(k)$ is the model output without time delay and $Y_{m2}(k)$ is the delayed model output.

It is well-known that a null steady state error is achieved both in the tracking of a step command and in the rejection of a step disturbance applied to the process input if an integral action is added to an SFC in the direct path [57,66]. Therefore, to guarantee a null steady state error of the error signal $e(k)$, a PI controller was added, which provides said integral action and has two gains whose tuning allows improving the performance of the control system.

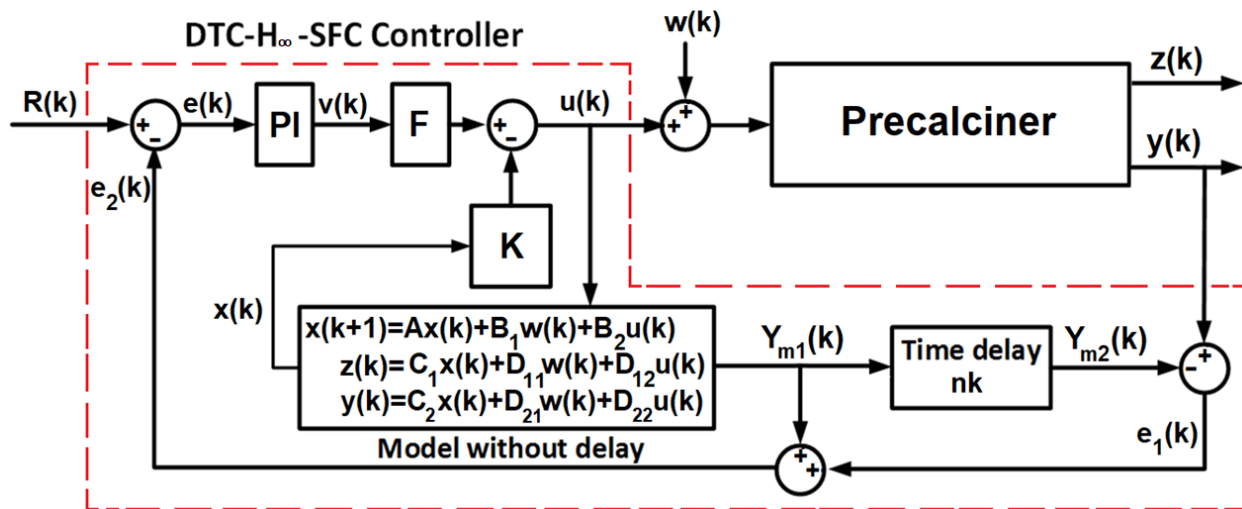


Figure 5. Diagram of the designed precalciner temperature control system with the designed DTC-H ∞ -SFC controller.

Consequently, the discrete-time PI controller is represented by the expression [67]:

$$v(k) = K_C e(k) + K_I e(k) + P_I(k-1) \quad (13)$$

where

$$P_I(k) = K_I \sum_{j=0}^k e(j) = K_I e(k) + P_I(k-1) \quad (14)$$

K_C is the proportional gain, $K_I = \frac{K_C T_s}{T_I}$ is the integral gain, T_I is the integral time constant. The state feedback control law is described by the expression [49]:

$$u(k) = -Kx(k) + Fv(k) \quad (15)$$

where $K \in \mathbb{R}^{1 \times 4}$ is the stabilizing controller, and $F \in \mathbb{R}^{1 \times 1}$ is the tracking gain.

The next suppositions were considered:

- (i) (A, B_1) is stabilizable and (C_1, A) is detectable;
- (ii) (A, B_2) is stabilizable and (C_2, A) is detectable.

Supposition (i) guarantees that internal stability of P is equivalent to BIBO (bounded-input, bounded-output) stability from w to z .

Supposition (ii) is necessary and hopeful that P can be internally stabilized by output feedback.

The H ∞ problem is to meet a stabilizing controller K that minimizes the H ∞ -norm of the transfer function from w to z [50,57]. The tracking gain F permits the system output y to achieve the reference R by settling the non-zero reference tracking problem of the system being the error $e = R - y$. Here, it should be complied:

$$F = [C_2(I - (A - B_2K))^{-1}B_2]^{-1} \quad (16)$$

After inserting (15) into the discrete-time state space process model without time delay (12) it is obtained:

$$\begin{aligned} x(k+1) &= (A - B_2K)x(k) + B_2Fv(k) + B_1w(k) \\ z(k) &= (C_1 - D_{12}K)x(k) + D_{12}Fv(k) + D_{11}w(k) \end{aligned} \quad (17)$$

Thus, the controller K and the tracking gain F are determined as:

$$K = [K_{11} \ K_{12} \ K_{13} \ K_{14}], F = [f_{11}] \quad (18)$$

The transfer matrix from $w(k)$ to $z(k)$ is obtained by means of:

$$G_{w,z}(z) = (C_1 - D_{12}K)(zI - (A - B_2K))^{-1}B_1 + D_{11} \quad (19)$$

Considering the process dominant time delay ($nk = 10T_s = 600$ s) the use of a dead-time compensator is proposed to compensate said delay in the feedback [32,66].

Therefore, the H_∞ control problem studied in this work is specified as: to meet a controller K such that $(A - B_2K)$ is Hurwitz and $\|G_{w,z}\|_\infty < \gamma$ for the minimum value of $\gamma > 0$ that meets the following linear matrix inequality [50,57]:

$$\begin{bmatrix} (A - B_2K)X + X(A - B_2K)^T & B_1 & X(C_1 - D_{12}K)^T \\ B_1^T & -I & D_{11}^T \\ (C_1 - D_{12}K)X & D_{11} & -\gamma^2 I \end{bmatrix} < 0 \quad (20)$$

$$X > 0 \quad (21)$$

where, X is a symmetric matrix and γ is a given positive number.

From (20) it was obtained:

$$K = [-0.6982 \ -3.7307 \ -5.0445 \ -2.8008], \text{ and } F = [1] \quad (22)$$

Furthermore, as a result of tuning the PI controller, $K_C = 80$ and $K_I = 19.9$ were obtained.

3. Results and Discussion

To assess the performance and accuracy of the DTC- H_∞ -SFC controller designed for precalciner temperature control, some tests based on simulations of real industrial operating scenarios of the control system were developed.

The first test consisted of verifying the capacity of the DTC- H_∞ -SFC controller for tracking variations in the command signal $R(k)$. Figure 6 exhibits the time response of the control system with the DTC- H_∞ -SFC controller designed, as well as the control effort against a change in the command signal from 920 to 950 °C.

From Figure 6, it can be seen that the temperature in the precalciner reaches the new reference value in a time period of approximately 1245 s, without overshoot and with a steady state error $e(k) = 0$.

These results show that the designed DTC- H_∞ -SFC controller has sufficient capacity to effectively follow the variation in the command signal in a time period less than 1250 s, and, therefore, it is within the established limits of nominal operating temperature in the precalciner [6,11].

Considering that, currently, the PI and the DTC+PI are the most used controllers for precalciner temperature control of cement rotary kilns [30,31], the second test consisted of comparatively analysing the tracking capacity of the DTC- H_∞ -SFC vs. DTC+PI controllers to variations in the command signal, as well as the rejection of the negative effect of external disturbances in environments close to the nominal operating conditions of the precalciner under study. Therefore, a discrete-time DTC with PI (DTC+PI) controller was designed. For this reason, the model obtained from the temperature in the precalciner (6) was used as the internal model of the DTC. The parameters obtained from the tuning of this PI controller were: $K_C = 0.00575$ and $K_I = 0.0008225$.

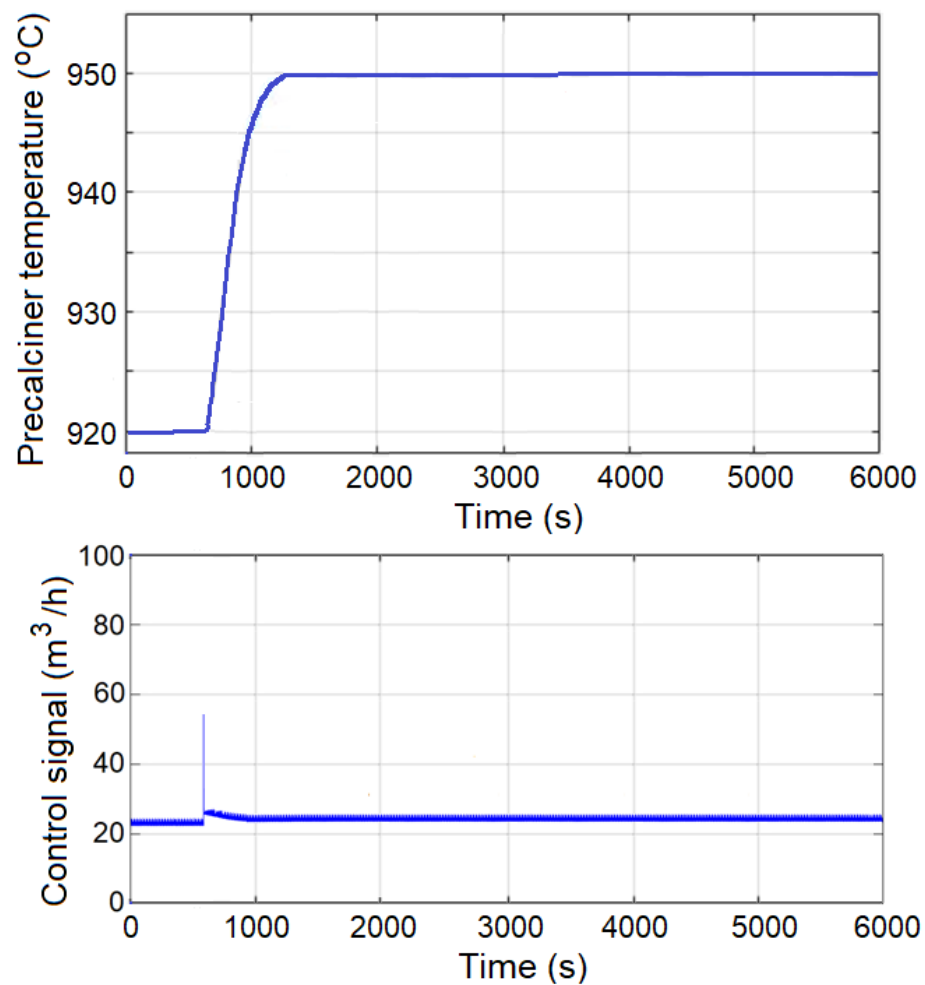


Figure 6. Time response of the control system with the DTC-H ∞ -SFC controller designed, as well as the control effort against a change in the command signal from 920 to 950 °C.

Figure 7 exhibits the time response of the control system with DTC-H ∞ -SFC vs. DTC+PI controllers against a change in the command signal from 910 to 950 °C. From said figure it can be observed that with the DTC-H ∞ -SFC controller the temperature in the precalciner reaches the reference value in a time period of approximately 1400 s, while with the PI controller the new reference is reached with overshoot and in a time period of 4000 s, that is, in a time interval 2.85 greater.

From Figure 7 it is also observed that in time $t = 4400$ s an external step-type disturbance $w(k)$ occurs due to a decrease in the opening magnitude of the control valve that regulates the fuel flow to the burner of the rotary kiln (see Figure 1), causing a decrease in said fuel flow of 5 m³/h. As a result, the hot gases that reach the precalciner (from the rotary kiln) decrease in temperature and cause a variation in the precalciner temperature. The DTC-H ∞ -SFC controller completely rejects this negative effect in a time period of approximately 800 s, while the PI refuses it in a time period of approximately 2300 s, that is in a time interval 2.87 larger.

These results show that the DTC-H ∞ -SFC controller designed has sufficient capacity to effectively reject the negative effects of external disturbances within the established limits of nominal operation of the precalciner temperature.

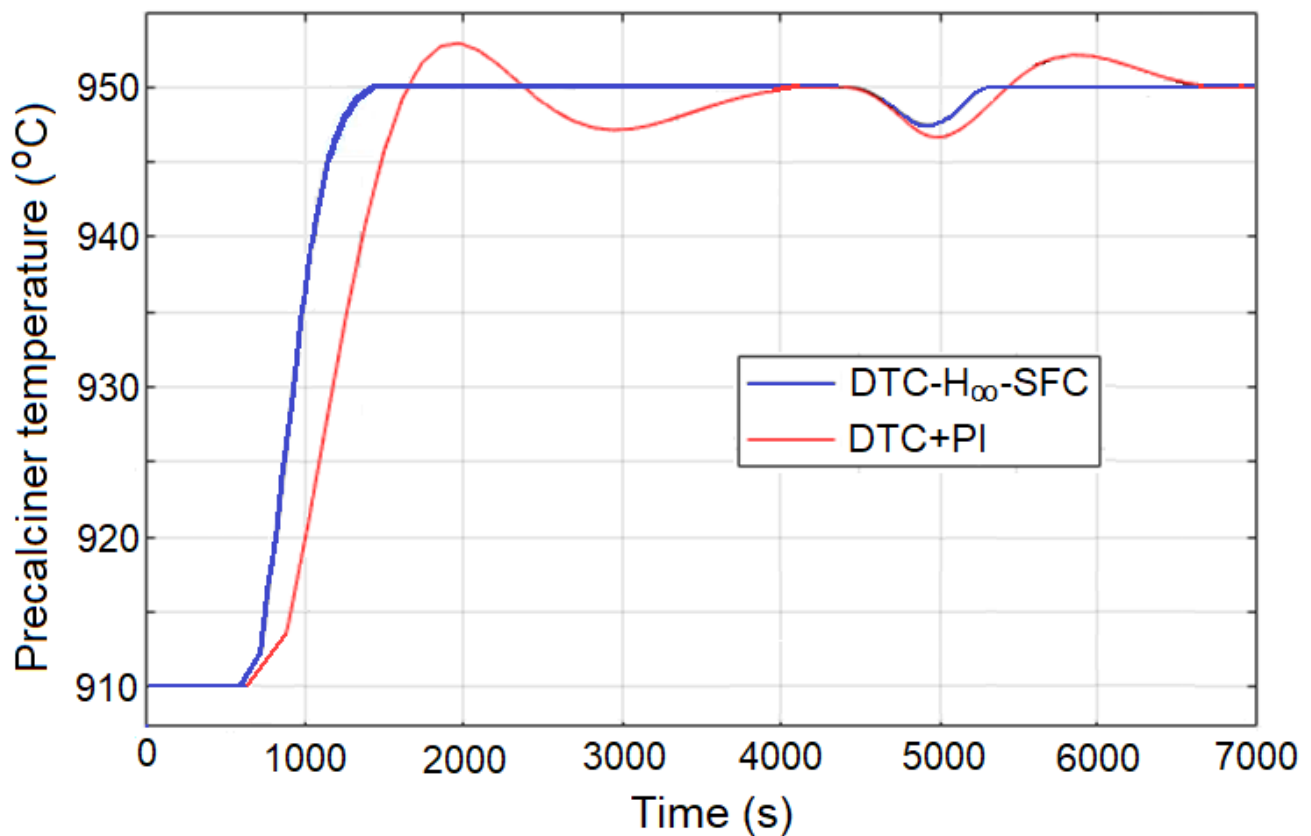


Figure 7. Performance comparative results of the control system with DTC- H_{∞} -SFC vs. DTC+PI controllers against variations in the command signal, and external disturbance.

To assess the performance of the control system with the controllers designed, the performance indexes of the integral squared error (ISE) and the integral absolute error (IAE) were used, which are represented by the following expressions [67]:

$$J_{ISE} = \sum_{k=0}^N e(k)^2 \quad (23)$$

$$J_{IAE} = \sum_{k=0}^N |e(k)| \quad (24)$$

Tables 2 and 3 show the comparative results of the ISE and IAE performance indices defined in (23), (24) of the temperature control system in the precalciner with the DTC- H_{∞} -SFC vs. DTC+PI controllers, considering the effect of an external disturbance. Again, the results obtained show that the DTC- H_{∞} -SFC controller allows for significantly better performance of the control system because it exhibits a lower ISE and a lower IAE.

Table 2. Comparative results of integral squared error (ISE) performance index of the control system with the DTC- H_{∞} -SFC and DTC+PI designed controllers and external disturbance.

	ISE (NOMINAL)	ISE (DISTURBANCE)
DTC+PI	14,149	140
DTC- H_{∞} -SFC	13,230	45

Table 3. Comparative results of integral absolute error (IAE) performance index of the control system with the DTC-H ∞ -SFC and DTC+PI designed controllers and external disturbance.

	IAE (NOMINAL)	IAE (DISTURBANCE)
DTC+PI	302	42
DTC-H ∞ -SFC	277	17

Therefore, the DTC-H ∞ -SFC designed controller provides important improvements in the precalciner temperature control of the cement rotary kiln, producing higher rank cement with lower energy consumption, and with lower emission of polluting gases.

4. Conclusions

Based on experimental real time data and system identification tools, a mathematical model that adequately defines the dynamic behaviour of temperature in a precalciner was obtained. The obtained model is given in fourth order discrete-time and presents a dominant time delay.

A DTC-H ∞ -SFC controller was designed for the operative temperature control in a precalciner, which is distinguished by using a dead time compensator (DTC) to compensate the process time delay, and a state feedback H ∞ controller (H ∞ -SFC) modified by adding a PI controller to reject the negative effects of external disturbances.

The obtained simulation results revealed that the DTC-H ∞ -SFC designed controller exhibits sufficient capacity to effectively track variations in the command signal and reject the negative effects of external disturbances in the time periods that are within the established nominal operating limits of the precalciner temperature.

The results of the comparative evaluation of the DTC-H ∞ -SFC vs. DTC+PI designed controllers, through the indexes of the integral squared error (ISE), and integral absolute error (IAE), showed that the DTC-H ∞ -SFC gives significantly better performance of the control system.

The next stage of our research involves the application of the DTC-H ∞ -SFC designed controller in the precalciner of the rotary kiln of the company Cementos Lima.

Author Contributions: J.S.-M. develops the experiments, R.R.-P. the mathematical model, and J.S.-H. the complete ideas of the exposed research. All authors have read and agreed to the published version of the manuscript.

Funding: This research received no external funding.

Institutional Review Board Statement: Not applicable.

Informed Consent Statement: Not applicable.

Data Availability Statement: Not applicable.

Acknowledgments: This paper was developed based on the technical information and data obtained from a precalciner of Cementos Lima company, Peru.

Conflicts of Interest: The authors declared no conflict of interest.

References

1. Udugu, A.A.; Khare, A. Automation of cement industries. *Int. J. Res. Eng. Adv. Technol.* **2014**, *1*, 1–5.
2. Samanta, A.; Chowdhury, A.; Dutta, A. Process automation of cement plant. *Int. J. Inform. Technol. Control Automat.* **2012**, *2*, 63–72. [\[CrossRef\]](#)
3. Rodrigues, F.A.; Joeke, I. Cement industry: Sustainability, challenges and perspectives. *Environ. Chem. Lett.* **2011**, *9*, 151–166. [\[CrossRef\]](#)
4. Poudyal, L.; Adhikari, K. Environmental sustainability in cement industry: An integrated approach for green and economical cement production. *Resour. Environ. Sustain.* **2021**, *4*, 100024. [\[CrossRef\]](#)
5. Deolalkar, S.P. *Handbook for Designing Cement Plants*; BS Publications: Hyderabad, India, 2021.
6. Alsop, P.A. *The Cement Plant Operations Handbook*, 6th ed.; Tradership Publication LTD.: Surrey, UK, 2014.

7. Millera, S.A.; John, V.M.; Paccac, S.A.; Horvath, A. Carbon dioxide reduction potential in the global cement industry by 2050. *Cem. Concr. Res.* **2018**, *114*, 115–124. [\[CrossRef\]](#)
8. Atmaca, A.; Yumrutas, R. Analysis of the parameters affecting energy consumption of a rotary kiln in cement industry. *Appl. Therm. Eng.* **2014**, *66*, 435–444. [\[CrossRef\]](#)
9. Schneider, M. The cement industry on the way to a low-carbon future. *Cem. Concr. Res.* **2019**, *124*, 105792. [\[CrossRef\]](#)
10. Boateng, A.A. *Rotary Kilns Transport Phenomena and Transport Processes*; Butterworth-Heinemann: Oxford, UK, 2008.
11. Peray, K.E. *The Rotary Cement Kiln*, 2nd ed.; Chemical Publishing Co. Inc.: New York, NY, USA, 1986.
12. Goshayeshi, H.R.; Poo, F.K. Modeling of rotary kiln in cement industry. *J. Energy Power Eng.* **2016**, *8*, 23–33. [\[CrossRef\]](#)
13. Salcedo Hernández, J.; Rivas-Perez, R.; Sotomayor Moriano, J.J. Design of a generalized predictive controller for temperature control in a cement rotary kiln. *IEEE Lat. Am. Trans.* **2018**, *16*, 1015–1021. [\[CrossRef\]](#)
14. Stadler, K.S.; Poland, J.; Gallestey, E. Model predictive control of a rotary cement kiln. *Control Eng. Pract.* **2011**, *19*, 1–9. [\[CrossRef\]](#)
15. Feliu-Batlle, V.; Rivas-Perez, R. Design of a robust fractional order controller for burning zone temperature control in an industrial cement rotary kiln. *IFAC-PapersOnLine* **2020**, *53*, 3657–3662. [\[CrossRef\]](#)
16. Teja, R.; Sridhar, P.; Guruprasath, M. Control and optimization of a triple string rotary cement kiln using model predictive control. *IFAC-PapersOnLine* **2016**, *49*, 748–753. [\[CrossRef\]](#)
17. Salcedo Hernández, J.; Rivas-Perez, R.; Sotomayor Moriano, J.J. Model reference adaptive temperature control of a rotary cement kiln. In Proceedings of the 2018 IEEE PES Transmission & Distribution Conference and Exhibition—Latin America, Lima, Peru, 18–21 September 2018; pp. 1–4.
18. King, R. Intelligent control in the cement industry. *IFAC Proc. Vol.* **1988**, *21*, 303–307. [\[CrossRef\]](#)
19. Salcedo Hernández, J.; Rivas-Perez, R. Model based predictive control of temperature in a cement rotatory kiln. *Electro-Electrónica* **2010**, *34*, 52–60.
20. Koumboulis, F.N.; Kouvakas, N.D. Indirect adaptive neural control for precalcination in cement plants. *Math. Comput. Simul.* **2002**, *60*, 325–334. [\[CrossRef\]](#)
21. Griparis, M.K.; Koumboulis, F.N.; Machos, N.S.; Marinos, J. Precalcination in cement plants (system descriptions and control trends). *IFAC Proc. Vol.* **2000**, *33*, 273–278. [\[CrossRef\]](#)
22. Camdali, U.; Erisen, A.; Celen, F. Energy and exergy analyses in a rotary kiln with pre-calcinations in cement production. *Energy Convers. Manag.* **2004**, *45*, 3017e3031. [\[CrossRef\]](#)
23. Li, S.; Ge, Y.; Wei, X. Experiment on NOx reduction by advanced reburning in cement precalciner. *Fuel* **2018**, *224*, 235–240. [\[CrossRef\]](#)
24. Stadler, K.S.; Wolf, B.; Gallestey, E. Precalciner control in the cement production process using MPC. *IFAC Proc. Vol.* **2007**, *40*, 201–206. [\[CrossRef\]](#)
25. Salcedo Hernández, J.; Feliu Battle, V.; Rivas-Perez, R. State feedback temperature control based on a Smith predictor in a precalciner of a cement kiln. *IEEE Lat. Am. Trans.* **2021**, *19*, 138–146.
26. Yang, B.; Cao, D. Action-dependent adaptive critic design based neurocontroller for cement precalciner kiln. *Int. J. Comput. Netw. Inf. Secur.* **2009**, *1*, 60–67. [\[CrossRef\]](#)
27. Stadler, K.S.; Wolf, B.; Gallestey, E. Model predictive control of the calciner at Holcim's Lägerdorf plant. *ZKG Int.* **2007**, *60*, 60–67.
28. Valarmathi, R.; Guruprasath, M.; Ramkumar, K. Design and implementation of evolutionary algorithm based controller for calciner process. *Int. J. Pure Appl. Math* **2017**, *117*, 711–723.
29. Osmic, J.; Omerdic, E.; Imsirovic, E.; Smajlovic, T.O.; Omerdic, E. Identification and control of precalciner in the cement plant. In Proceedings of the 14th APCA International Conference on Automatic Control and Soft Computing, Bragança, Portugal, 1–3 July 2020; pp. 126–135.
30. Tsamatsoulis, D.C.; Zlatev, G. PID parameterization of cement kiln precalciner based on simplified modeling. *Int. J. Neural Netw. Adv. Appl.* **2016**, *3*, 41–45.
31. Mohankrishna, P.B.; Vigneshwaran, S.; Padmadarshan, M.B.; Brijet, Z. Fuzzy based PID for calciner temperature control. *Int. J. Pure Appl. Math.* **2018**, *119*, 14563–14570.
32. Normey-Rico, J.E.; Camacho, E.F. *Control of Dead-Time Processes*; Springer: London, UK, 2007.
33. Kao, T.G.; Nguen, M.; Rivas-Perez, R. Adaptive control of a delay plant by using a nonsearching self-adjusting systems with a model. *Autom. Telemekh.* **1988**, *12*, 106–116.
34. Wang, Z.; Yuan, M.; Wang, B.; Wang, H.; Wang, T. Dynamic model of cement precalcination process. In Proceedings of the 27th IASTED International Conference on Modeling, Identification, and Control, Innsbruck, Austria, 11–13 February 2008; pp. 352–357.
35. Tsamatsoulis, D.C. Simplified modeling of cement kiln precalciner. *Int. J. Mater.* **2016**, *3*, 69–73.
36. Fellaou, S.; Harnoune, A.; Seghra, M.A.; Bounahmidi, T. Statistical modeling and optimization of the combustion efficiency in cement kiln precalciner. *Energy* **2018**, *155*, 351–359. [\[CrossRef\]](#)
37. Fidaros, D.K.; Baxevanou, C.A.; Dritselis, C.D.; Vlachos, N.S. Numerical modelling of flow and transport processes in a calciner for cement production. *Powder Technol.* **2007**, *171*, 81–85. [\[CrossRef\]](#)
38. Kovalienko, P.I.; Matzeliuk, E.M.; Rivas-Perez, R. Adaptive control of water distribution in main irrigation canals with variable time delay. *Sci. Res. Hydrotech. Land Reclam.* **1990**, 32–40.
39. Acedo Sánchez, J. *Control Avanzado de Procesos, Teoría y Práctica*; Ediciones Díaz de Santos, S.A.: Madrid, España, 2009.

40. Rivas-Perez, R. Technological Process Control in Main Canals of Irrigation Systems, with Application to Irrigation Systems of Cuba. Ph.D. Thesis, Scientific Research Institute on Land Reclamation and Hydraulic Engineering of Ukrainian Academy of Agricultural Sciences (UkrNIIGIM), Kiev, Ukraine, 1984.
41. Visioli, A. *Practical PID Control*; Springer: London, UK, 2006.
42. Calderon Mendoza, E.M.; Rivas-Perez, R.; Sotomayor-Moriano, J.J. Design of neuro-fuzzy controller for control of water distribution in an irrigation main canal. *IEEE Lat. Am. Trans.* **2016**, *14*, 471–476. [[CrossRef](#)]
43. Astrom, K.; Hagglund, T. *Advanced PID Control*; Pearson Education, S.A.: Madrid, Spain, 2009.
44. Fridman, E. *Introduction to Time-Delay Systems Analysis and Control*; Springer International Publishing: Cham, Switzerland, 2014.
45. Sanz, R.; García, P.; Albertos, P. A generalized Smith predictor for unstable time-delay SISO systems. *ISA Trans.* **2018**, *72*, 197–204. [[CrossRef](#)] [[PubMed](#)]
46. Rivas-Perez, R. Synthesis of optimal stationary automatic control systems of water distribution in main irrigation canals by means of time delay compensation. *Land Reclam. Water Manag.* **1991**, *74*, 77–82.
47. Richter, H. *Advanced Control of Turbofan Engines*; Springer: Cleveland, OH, USA, 2012.
48. Rodriguez Vasquez, J.R.; Rivas-Perez, R.; Sotomayor-Moriano, J.J.; Peran-González, J.R. Advanced control system of the steam pressure in a fire-tube boiler. *IFAC Proc. Vol.* **2008**, *41*, 11028–11033. [[CrossRef](#)]
49. Zhou, K.; Doyle, J. *Essentials of Robust Control*; Pearson Education: Upper Saddle River, NJ, USA, 1999.
50. Gu, D.W.; Petko, H.P.; Konstantinov, M.M. *Robust Control Design with MATLAB®*, 2nd ed.; Springer: London, UK, 2013.
51. Sánchez-Peña, R.; Sznajder, M. *Robust Systems Theory and Applications*; Wiley-Interscience: New York, NY, USA, 2008.
52. Normey-Rico, J.E.; Camacho, E.F. Dead-time compensators: A survey. *Control Eng. Pract.* **2008**, *16*, 407–428. [[CrossRef](#)]
53. Feliu-Batlle, V.; Rivas-Perez, R. Control of the temperature in a petroleum refinery heating furnace based on a robust modified Smith predictor. *ISA Trans.* **2021**, *12*, 251–270. [[CrossRef](#)]
54. Zhou, K.; Doyle, J.; Glover, K. *Robust and Optimal Control*; Prentice Hall: New Jersey, NJ, USA, 1996.
55. Feliu-Batlle, V.; Rivas-Perez, R.; Sanchez-Rodriguez, L.; Castillo-García, F.J.; Linarez Saez, A. Robust fractional order PI controller for a main irrigation canal pool. *IFAC Proc. Vol.* **2008**, *41*, 15535–15540. [[CrossRef](#)]
56. Stoorvogel, A. *The H_∞ Control Problem: A State-Space Approach*; Prentice Hall: New Jersey, NJ, USA, 1992.
57. Morari, M.; Zafiroiu, E. *Robust Process Control*; Prentice Hall: New Jersey, NJ, USA, 1989.
58. Benitez, I.O.; Rivas, R.; Feliu, V.; Castillo, F.J. Temperature control based on a modified Smith predictor for injectable drug formulations. *IEEE Lat. Am. Trans.* **2015**, *13*, 1041–1047. [[CrossRef](#)]
59. Fridman, L.; Poznyak, A.; Bejarano, F.J. *Robust Output LQ Optimal Control via Integral Sliding Modes*; Springer: New York, NY, USA, 2014.
60. Salcedo-Hernández, J.; Rivas-Perez, R.; Sotomayor-Moriano, J. Design of a robust H2 state feedback temperature controller for a steel slab reheating furnace. *Appl. Sci.* **2020**, *10*, 1731. [[CrossRef](#)]
61. Dolly Mary, A.; Mathew, A.T.; Jacob, J. Robust H-infinity (H_∞) stabilization of uncertain wheeled mobile robots. *Glob. J. Res. Eng. Electric. Electron. Eng.* **2012**, *12*, 090602.
62. Ljung, L. System Identification. In *Theory for the User*; Prentice-Hall: Hoboken, NJ, USA, 1999.
63. Inoue, M.; Wada, T.; Ikeda, M.; Uezato, E. State-space H_∞ controller design for descriptor systems. *Automatica* **2015**, *59*, 164–170. [[CrossRef](#)]
64. Xu, S.; Chen, T. Robust H_∞ control for uncertain discrete-time systems with time-varying delays via exponential output feedback controllers. *Systems Control Lett.* **2004**, *51*, 171–183. [[CrossRef](#)]
65. Kailath, T. *Linear Systems*; Prentice Hall: New Jersey, NJ, USA, 1980.
66. Rivas-Perez, R.; Cao, T.H.; Pichuguin, E.D.; Nguen, V.D. State space reconstruction in multivariable plants with time-delay. *Control Cibernética Y Autom.* **1989**, *22*, 30–35.
67. Ogata, K. *Discrete-Time Control System*, 2nd ed.; Prentice-Hall International Inc.: New Jersey, NJ, USA, 1995.